Journal of Power Sources 244 (2013) 625–630

Contents lists available at SciVerse ScienceDirect

Journal of Power Sources

journal homepage: www.elsevier.com/locate/jpowsour

Short communication

Characteristics of stabilized spinel cathode powders obtained by in-situ coating method

Young Jun Hong [a], Mun Yeong Son [a], Jung-Kul Lee [a], Hyung Bok Lee [b], Seong Ho Lee [b], Yun Chan Kang [a,*]

[a] Department of Chemical Engineering, Konkuk University, 1 Hwayang-dong, Gwangjin-gu, Seoul 143-701, Republic of Korea
[b] Advanced Battery Development Team, Battery R&D, Global Technology, SK Innovation 325, Exporo, Yuseong-gu, Daejeon 305-712, Republic of Korea

HIGHLIGHTS

- TiO_2-coated $LiMn_2O_4$ cathode powders are prepared using an in situ spray pyrolysis process.
- The single-crystalline $LiMn_2O_4$ primary particles are uniformly coated with an amorphous TiO_2 layer.
- The capacity retentions of the pure and TiO_2-coated $LiMn_2O_4$ powders are 69% and 86% of the initial capacity after 170 cycles.

GRAPHICAL ABSTRACT

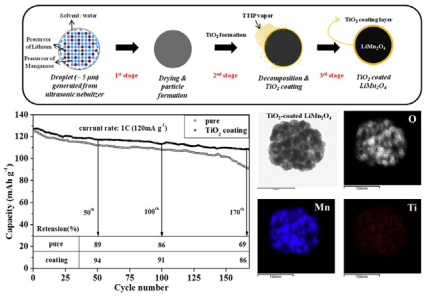

ARTICLE INFO

Article history:
Received 15 October 2012
Received in revised form
28 November 2012
Accepted 3 January 2013
Available online 16 January 2013

Keywords:
Cathode material
Spray pyrolysis
Surface coating
Lithium manganate

ABSTRACT

TiO_2-coated $LiMn_2O_4$ cathode powders are prepared using an in situ spray pyrolysis process. The TiO_2-coated $LiMn_2O_4$ powders have spherical aggregated structures of nanometer-sized primary particles. The mean sizes of the primary and secondary TiO_2-coated $LiMn_2O_4$ powders are 55 and 880 nm, respectively. The transmission electron microscopy images of the $LiMn_2O_4$ primary particles show a single-crystalline and well-faceted structure. The single-crystalline $LiMn_2O_4$ primary particles are uniformly coated with an amorphous TiO_2 layer. An immediate reaction of titanium tetraisopropoxide with oxygen forms a small flame at the exit of an alumina tube located in the center part of a quartz reactor. Sudden collisions between TiO_2 vapor and submicron-sized composite powders of the Li and Mn components occur to form the TiO_2-coated cathode powders. The discharge capacities of the TiO_2-coated $LiMn_2O_4$ cathode powders are 126 and 109 mAh g^{-1} in the first and 170 cycles at a current density of 1 C. The capacity retentions of the pure and TiO_2-coated $LiMn_2O_4$ powders are 69% and 86% of the initial capacity after 170 cycles.

1. Introduction

Li–Mn spinel has advantages as the cathode material in Li-ion secondary batteries, such as low cost, high abundance, high safety, ease of preparation, and nontoxicity [1–5]. However, since it suffers from capacity fading during cycling for several reasons, including dissolution of Mn ions into the electrolyte and a phase transition caused by Jahn–Teller distortion, its applications are limited [6,7].

Surface modification by stable oxide materials has proven to be effective in improving the electrochemical properties of $LiMn_2O_4$ powders [8–11]. A stable oxide coating layer on the surface of the cathode material improved electrochemical properties and thermal stability compared to those of the uncoated system. The coating materials prevented contact between the cathode material and the

* Corresponding author. Tel.: +82 2 2049 6010; fax: +82 2 458 3504.
E-mail address: yckang@konkuk.ac.kr (Y.C. Kang).

0378-7753/$ – see front matter © 2013 Elsevier B.V. All rights reserved.
http://dx.doi.org/10.1016/j.jpowsour.2013.01.024

electrolyte and changes in the cathode phase. The electrochemical properties of the coated $LiMn_2O_4$ cathode powders were affected by the type of oxide material as well as the method used for formation of the oxide coating layer [12–14]. In previous reports, metal-oxide-coated $LiMn_2O_4$ powders were mainly prepared using a two-step process. The prepared $LiMn_2O_4$ powders were coated with stable oxide materials via various liquid-solution methods [15,16]. A one-step process for the preparation of surface-modified cathode powders would be advantageous with respect to production costs.

Spray pyrolysis, which is a gas-phase-reaction method, has been applied to the preparation of spinel $LiMn_2O_4$ cathode powders with spherical morphologies, fine sizes, and good electrochemical properties [17–24]. However, surface modification of the cathode powders with an oxide material has rarely been performed using in situ spray pyrolysis. Choi et al. reported the characteristics of LBO glass-modified $LiMn_2O_4$ cathode powders prepared by spray pyrolysis [23]. LBO glass-modified $LiMn_2O_4$ cathode powders were prepared directly by spray pyrolysis from a spray solution containing the glass components. Modification with LBO glass improved the electrochemical properties as well as the morphological characteristics of the $LiMn_2O_4$ cathode powders. In this study, TiO_2-modified $LiMn_2O_4$ cathode powders were prepared by in situ spray pyrolysis. Titanium tetraisopropoxide (TTIP) vapor, used as the source material for TiO_2, was continuously supplied to the inner part of a quartz reactor to prepare coated $LiMn_2O_4$ powders by in situ spray pyrolysis. The uniform coating of TiO_2 stabilized the spinel cathode powders in cycling at high operating voltages.

2. Experimental

A schematic diagram of the large-scale in situ spray pyrolysis system used in this study is shown in Fig. 1. The equipment consisted of twenty ultrasonic spray generators operating at 1.7 MHz, TTIP evaporator, a tubular quartz reactor, and a bag filter. Appropriate amounts of TTIP vapors were continuously formed in a heating mental, maintained at 150 °C, by supplying a diluted TTIP solution (TTIP + absolute alcohol), using a peristaltic pump. The TTIP vapor was transferred to the second-stage quartz-reactor, maintained at 900 °C, through a small-radius alumina tube using high-purity argon gas. An immediate reaction of TTIP with oxygen formed a small flame at the exit of the alumina tube located in the center part of the quartz reactor. The length and diameter of the quartz reactor were 2000 and 100 mm, respectively. The reactor temperature was maintained at 900 °C. The flow rates of the air and argon used as the carrier gas were each 50 and 2 L min^{-1}. An aqueous spray solution was prepared by dissolving lithium nitrate ($LiNO_3$, Junsei) and manganese nitrate hexahydrate [$Mn(NO_3)_2.6H_2O$, Junsei] in distilled water. The amount of lithium added to the spray solution was in excess of 5 wt% of the stoichiometric amount to facilitate the formation of $LiMn_2O_4$ powders. The precursor particles obtained by ultrasonic spray pyrolysis were post-treated at a temperature of 600 °C for 3 h in an air atmosphere.

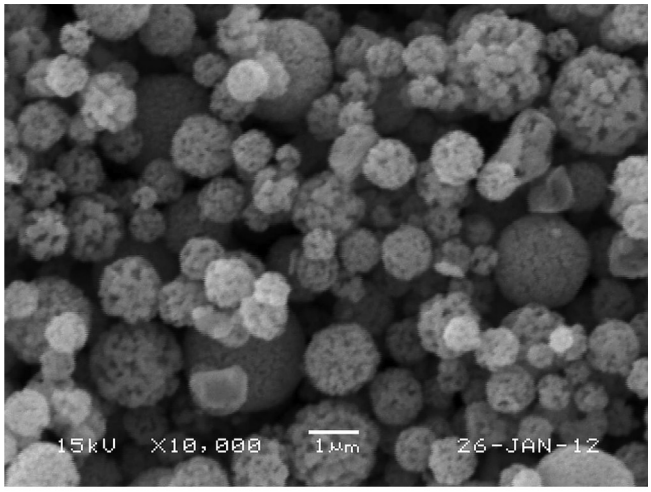

(a) pure $LiMn_2O_4$

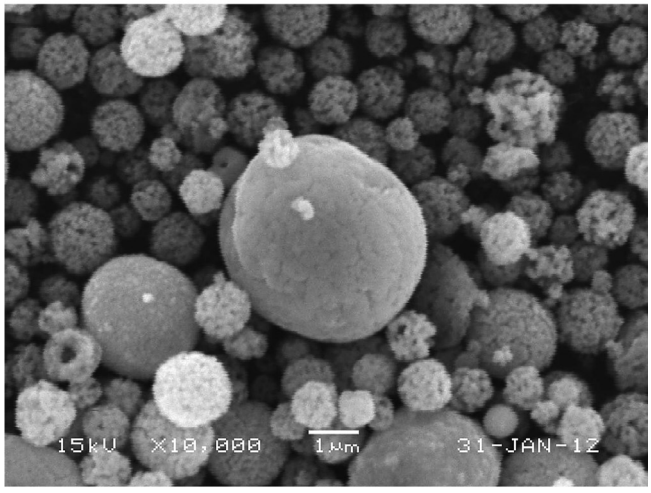

(b) TiO_2-coated $LiMn_2O_4$

Fig. 2. SEM images of the $LiMn_2O_4$ precursor powders prepared by spray pyrolysis.

The crystal structures of the prepared cathode powders were investigated using X-ray diffractometry (XRD; RIGAKU DMAX-33)

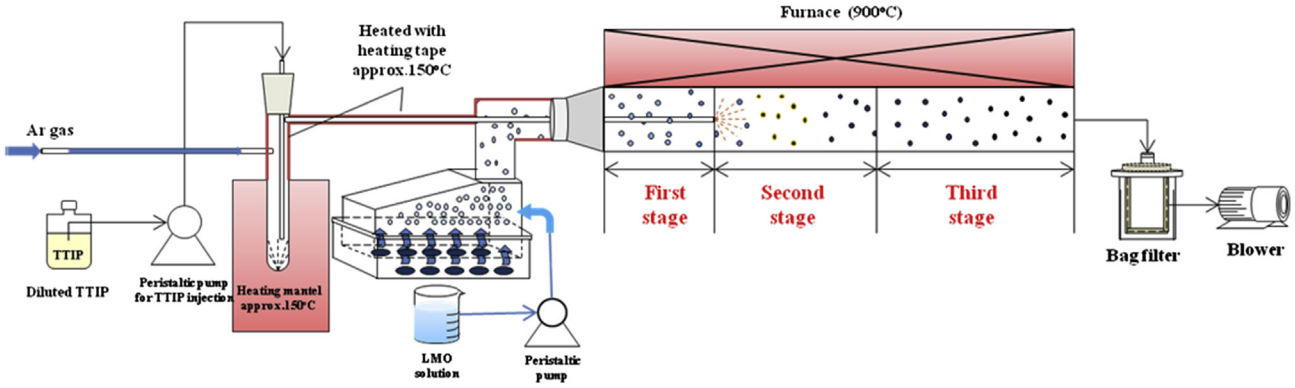

Fig. 1. Schematic diagram of the large-scale in situ spray pyrolysis process.

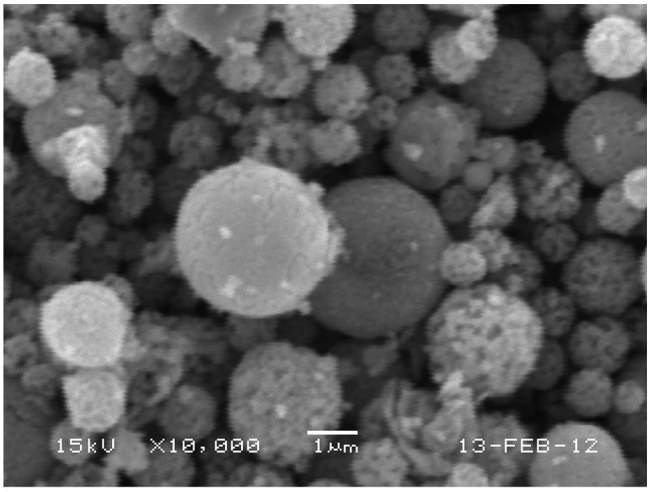

(a) pure $LiMn_2O_4$

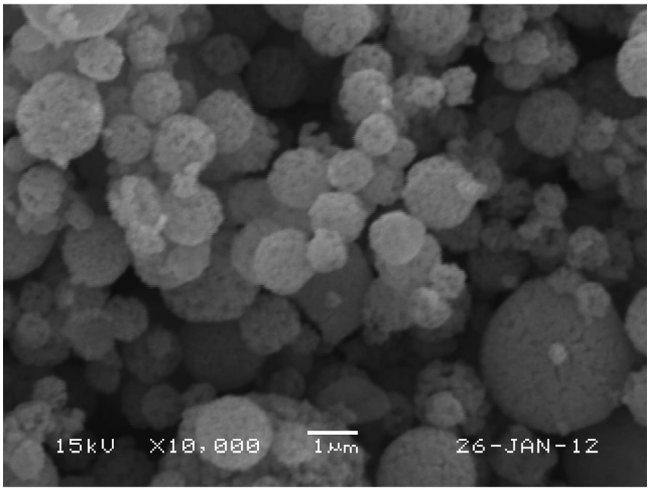

(b) TiO_2-coated $LiMn_2O_4$

Fig. 3. SEM images of the $LiMn_2O_4$ powders post-treated at 600 °C.

with Cu Kα radiation ($\lambda = 1.5418$ Å). The morphological characteristics of the powders were investigated using scanning electron microscopy (SEM; JEOL JSM-6060) and transmission electron microscopy (TEM, JEOL, JEM-2010). The capacities and cycle properties of the powders were determined by using a 2032-type coin cell. The cathode electrode was prepared from a mixture containing 20 mg of $LiMn_2O_4$ and 12 mg of TAB (TAB is a mixture of 9.6 mg of teflonized acetylene black and 2.4 mg of a binder). Lithium metal and microporous polypropylene film were used as the anode electrode and separator, respectively. The electrolyte was 1 M $LiPF_6$ in a 1:1 mixture by volume of ethylene carbonate/dimethyl carbonate (EC/DMC). The charge/discharge characteristics of the samples were determined through cycling in the 3.2–4.5 V potential range at a constant current density of 1 C (120 mA g^{-1}).

3. Results and discussion

The morphologies of the pure and TiO_2-coated $LiMn_2O_4$ powders before and after post-treatment are shown in Figs. 2 and 3. The cathode powders prepared directly by large-scale spray pyrolysis were spherical and had porous structures, regardless of the presence of the TiO_2 coating material. A spherical aggregated structure of nanometer-sized primary particles is a well-known morphology of $LiMn_2O_4$ powders prepared by spray pyrolysis [23,24]. One cathode particle was formed from one droplet by drying, decomposition, and crystallization processes. The mean sizes of the pure and TiO_2-coated $LiMn_2O_4$ powders, measured from the SEM images, were each 0.8 μm. The cathode powders prepared directly by large-scale spray pyrolysis at a short residence time of 3.8 s had low capacities and poor cycling properties because of low crystallinity and phase inhomogeneity. The cathode powders were therefore

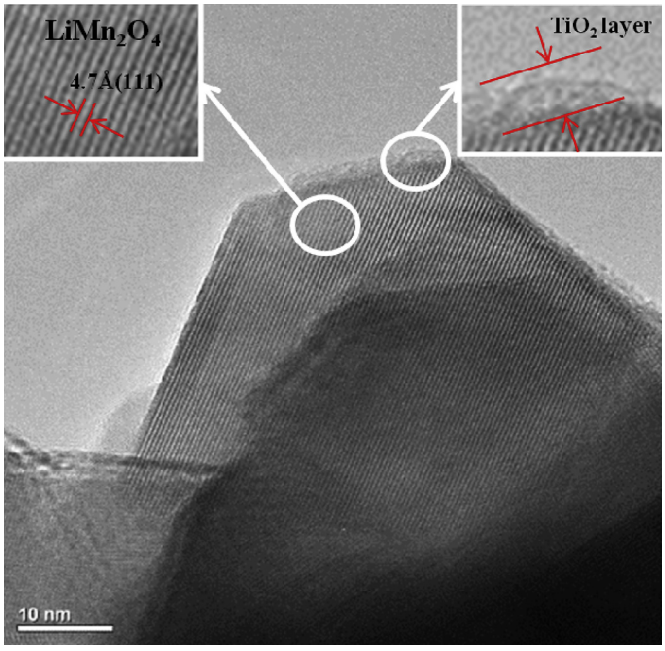

Fig. 5. High resolution TEM images of the TiO_2-coated $LiMn_2O_4$ powders post-treated at 600 °C.

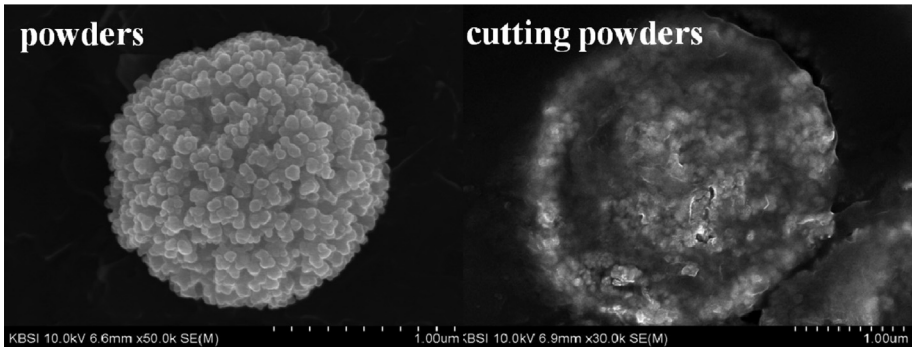

Fig. 4. High resolution SEM images of the TiO_2-coated $LiMn_2O_4$ powders and the surfaces of the cutting powders.

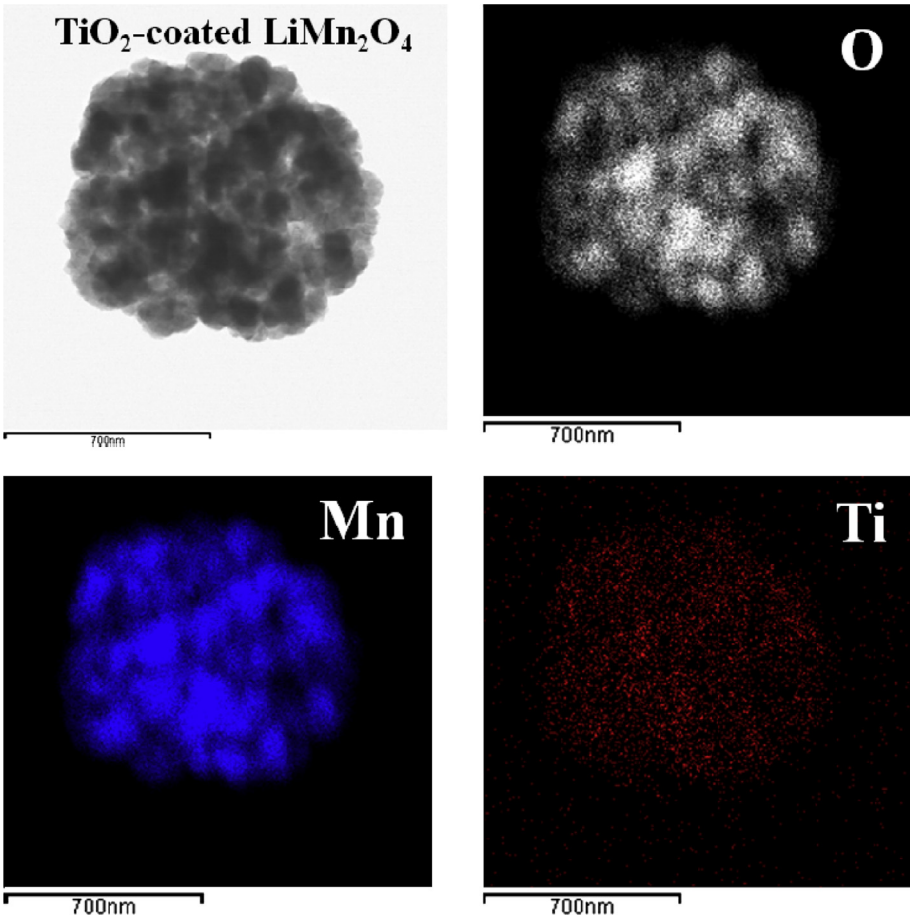

Fig. 6. EDS maps of the of the TiO_2-coated $LiMn_2O_4$ powders post-treated at 600 °C.

post-treated at 600 °C for 3 h to improve the electrochemical properties of the pure and TiO_2-coated $LiMn_2O_4$ powders. The post-treatment of the cathode powders did not change the spherical aggregated structure of the nanometer-sized primary particles of the $LiMn_2O_4$ powders.

Fig. 4 shows the high-resolution SEM images of the TiO_2-coated $LiMn_2O_4$ powders and the surfaces of the cutting powders. The mean size of the primary particles of the submicron-sized powders after post-treatment at 600 °C was 55 nm, and the cutting powders had filled and porous internal structures. Fig. 5 shows high-resolution TEM images of the post-treated TiO_2-coated $LiMn_2O_4$ powders. The TEM image of the $LiMn_2O_4$ primary particles shows a single-crystalline and well-faceted structure. The high-resolution TEM images show clear lattice fringes with a separation of 0.47 nm. This value corresponds to the (111) plane of the cubic lattice of $LiMn_2O_4$. The single-crystalline $LiMn_2O_4$ primary particles were coated with an amorphous TiO_2 layer, indicated by arrows in the TEM images. Crystallization of the TiO_2 layer did not occur at a post-treatment temperature of 600 °C. Fig. 6 shows the results of dot mapping of the post-treated TiO_2-coated $LiMn_2O_4$ powders. The low-resolution TEM image also shows the porous and nanostructured morphologies of the powders. The Ti component was uniformly distributed over the entire porous $LiMn_2O_4$. TiO_2 nanopowders formed from the TiO_2 vapor by nucleation and growth mechanisms were not observed in the high- and low-resolution TEM images, as shown in Figs. 5 and 6. The TiO_2 vapors formed by decomposition of TTIP were therefore deposited on the surface of the $LiMn_2O_4$ powder to form an amorphous TiO_2 coating layer. The formation mechanism of the TiO_2-coated $LiMn_2O_4$ powder in the large-scale spray pyrolysis process is shown in Fig. 7. The drying and decomposition of liquid droplets formed by an ultrasonic nebulizer from an aqueous spray solution of Li and Mn components produced mixed composite

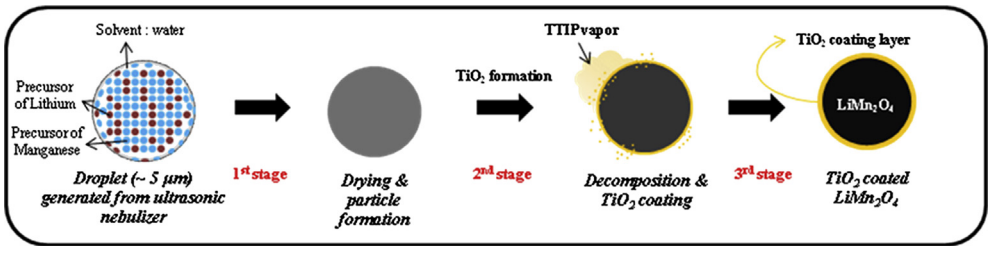

Fig. 7. Formation mechanism of the TiO_2-coated $LiMn_2O_4$ powders.

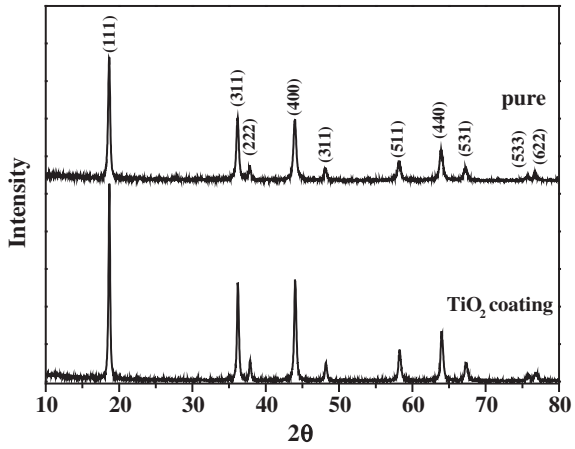

Fig. 8. XRD patterns of the pure and TiO_2-coated $LiMn_2O_4$ powders post-treated at 600 °C.

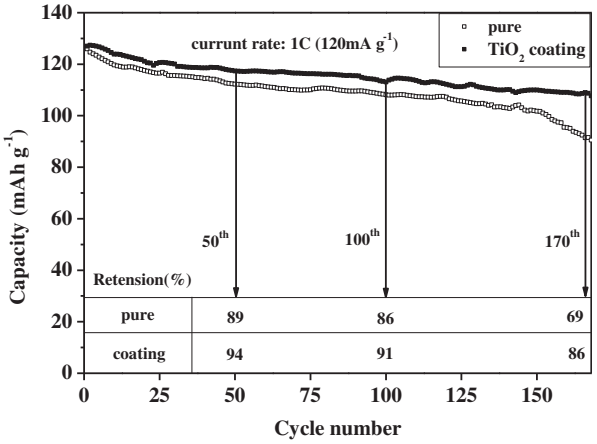

Fig. 10. Cycling properties of the pure and TiO_2-coated $LiMn_2O_4$ powders post-treated at 600 °C.

powders of Li and Mn components in the first stage. The composite powders were mixed in the gas phase with TiO_2 vapor in the second stage. The TTIP vapor was transferred to the second-stage quartz-reactor, maintained at 900 °C, through a small-radius alumina tube using high-purity argon gas. An immediate reaction of TTIP with oxygen formed a small flame at the exit of the alumina tube located in the center part of the quartz reactor. The sudden collision between TiO_2 vapor and submicron-sized composite powders of Li and Mn occurred to form TiO_2-coated composite powders. The reaction of the Li and Mn components to form the $LiMn_2O_4$ phase gradually occurred in all parts of the quartz reactor maintained at 900 °C. Consequently, TiO_2-coated $LiMn_2O_4$ powders of low crystallinity were prepared directly using a large-scale spray pyrolysis process.

Fig. 8 shows the XRD patterns of the pure and TiO_2-coated $LiMn_2O_4$ powders post-treated at 600 °C. The powders had pure cubic spinel $LiMn_2O_4$ crystal structures, regardless of the presence of the TiO_2 coating material. Impurity peaks originating from the Ti component were not observed in the XRD patterns. The mean crystallite sizes of the pure and TiO_2-coated $LiMn_2O_4$ powders, calculated using Scherrer's equation from the half-widths of the (111) XRD peaks, were 30 and 33 nm, respectively. The compositions of the TiO_2-coated $LiMn_2O_4$ powders were analyzed using ICP. The ratio of Li to Mn components in the cathode powder was similar to that of stoichiometric $LiMn_2O_4$. The content of TiO_2 was 0.02 wt% of the coated $LiMn_2O_4$ powders.

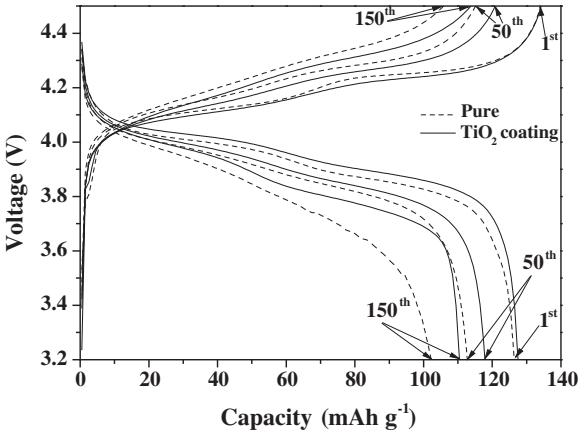

Fig. 9. Charge/discharge curves of the pure and TiO_2-coated $LiMn_2O_4$ powders post-treated at 600 °C.

Figs. 9 and 10 show the charge–discharge curves and the cycling properties of the post-treated pure and TiO_2-coated $LiMn_2O_4$ powders. The operating cut-off voltages were 3.2 and 4.5 V at a current density of 1 C (120 mA g^{-1}). The charge/discharge curves had similar shapes, regardless of the presence of the TiO_2 coating material. However, the cycling properties of the $LiMn_2O_4$ cathode powders were affected by the TiO_2 coating layer. The discharge capacities of the pure $LiMn_2O_4$ cathode powders were 126, 112, and 86 mAh g^{-1} in the first, 50th, and 170th cycles. The discharge capacities of the TiO_2-coated $LiMn_2O_4$ cathode powders were 126, 117, and 109 mAh g^{-1} in the first, 50th, and 170th cycles. The capacity retentions of the pure and TiO_2-coated $LiMn_2O_4$ powders were 69% and 86% of the initial capacity after 170 cycles. The bare and TiO_2-coated $LiMn_2O_4$ cathode powders were stored in vials containing electrolytes for 12 h at 80 °C. The amounts of Mn dissolution were 67 and 13 ppm for bare and TiO_2-coated $LiMn_2O_4$ cathode powders, respectively. The uniform TiO_2 coating layer improved the electrochemical properties of the spinel $LiMn_2O_4$ cathode powders by decreasing the dissolution of Mn ions into the electrolyte [25–27].

4. Conclusions

The effects of a TiO_2 coating layer on the electrochemical properties of $LiMn_2O_4$ powders prepared by large-scale spray pyrolysis are investigated. The TiO_2-coated $LiMn_2O_4$ powders are spherical, with filled and porous morphologies. TiO_2 vapor formed by decomposition of TTIP is transferred to the inner part of a quartz reactor maintained at 900 °C and deposits on the surface of the $LiMn_2O_4$ powder to form an amorphous TiO_2 coating layer. The sudden collision between TiO_2 vapor and submicron-sized composite powders of Li and Mn occurs, forming the TiO_2-coated composite powder in the gas phase. TiO_2-coated $LiMn_2O_4$ cathode powders prepared by in situ spray pyrolysis have high initial charge/discharge capacities and good cycling properties, even at a high current density. The uniform TiO_2 coating layer improves the electrochemical properties of the spinel $LiMn_2O_4$ cathode powders by decreasing the dissolution of Mn ions into the electrolyte.

Acknowledgements

This work was supported by the National Research Foundation of Korea (NRF) grant funded by the Korea government (MEST) (No. 2012R1A2A2A02046367). This study was supported by the Converging Research Center Program through the National Research Foundation of Korea (NRF) funded by the Ministry of Education,

Science and Technology (2011-50210). This work was supported by Seoul R&BD Program (WR090671).

References

[1] Y. Xia, Y. Zhou, M. Yoshio, J. Electrochem. Soc. 144 (1997) 2593.
[2] J.M. Tarascon, D. Guyomard, Electrochim. Acta 38 (1993) 1221.
[3] T. Ohzuku, M. Kitagawa, T. Hirai, J. Electrochem. Soc. 137 (1990) 769.
[4] J.M. Tarascon, M. Armand, Nature 414 (2001) 359.
[5] D. Guyomard, J.M. Tarascon, J. Electrochem Soc. 138 (1991) 2864.
[6] T. Aoshima, K. Okahara, C. Kiyohara, K. Shizuka, J. Power Sources 97-98 (2001) 377.
[7] D. Aurbach, M.D. Leve, B. Markovsky, G. Salitra, E. Levi, U. Heidra, L. Heidra, R. Oesten, J. Power Sources 81-82 (1999) 472.
[8] S.W. Lee, K.S. Kim, H.S. Moon, H.J. Kim, B.W. Cho, W.I. Cho, J.B. Ju, J.W. Park, J. Power Sources 126 (2004) 150.
[9] J. Cho, T.J. Kim, Y.J. Kim, B. Park, Chem. Commun. (2001) 1074.
[10] J. Tu, X.B. Zhao, G.S. Cao, D.G. Zhuang, T.J. Zhu, J.P. Tu, Electrochim. Acta 51 (2006) 6456.
[11] M.M. Thackeray, C.S. Johnson, J.S. Kim, Electrochem. Commun. 5 (2003) 752.
[12] Z. Chen, Y. Qin, K. Amine, Y.K. Sun, J. Mater. Chem. 20 (2010) 7606.
[13] J.S. Gnanaraj, V.G. Pol, A. Gedanken, D. Aurbach, Electrochem. Commun. 5 (2003) 940.
[14] Y.J. Park, J.G. Kim, M.K. Kim, H.T. Chung, W.S. Um, M.H. Kim, H.G. Kim, J. Power Sources 76 (1998) 41.
[15] J. Cho, G.B. Kim, H.S. Lim, C.S. Kim, S.I. Yoo, J. Electrochem. Soc. 12 (1999) 607.
[16] Z. Yang, W. Yang, D.G. Evans, Y. Zhao, X. Wei, J. Power Sources 189 (2009) 1147.
[17] S.H. Park, S.T. Myung, S.W. Oha, C.S. Yoon, Y.K. Sun, Electrochim. Acta 51 (2006) 4089.
[18] S.H. Ju, D.Y. Kim, E.B. Jo, Y.C. Kang, J. Mater. Sci. 42 (2007) 5369.
[19] I. Taniguchi, C.K. Lim, D. Song, M. Wakihara, Solid State Ionics 146 (2002) 239.
[20] I. Taniguchi, N. Fukuda, M. Konarova, Powder Technol. 181 (2008) 228.
[21] S.N. Karthick, S. Richard Prabhu Gnanakan, A. Subramania, H.J. Kim, J. Alloys Compd 489 (2010) 674.
[22] Z. Bakenov, I. Taniguchi, Solid State Ionics 176 (2005) 1027.
[23] S.H. Choi, J.H. Kim, Y.N. Ko, Y.J. Hong, Y.C. Kang, J. Power Sources 210 (2012) 110.
[24] S. Hirose, T. Kodera, T. Ogihara, J. Alloys Compd 506 (2010) 883.
[25] Y.K. Sun, C.S. Yoon, C.K. Kim, S.G. Youn, Y.S. Lee, M. Yoshio, I.H. Oh, J. Mater. Chem. 11 (2001) 2519.
[26] C. Li, H.P. Zhang, L.J. Fu, H. Liu, Y.P. Wua, E. Rahm, R. Holze, H.Q. Wu, Electrochim. Acta 51 (2006) 3872.
[27] Z.R. Zhang, H.S. Liu, Z.L. Gong, Y. Yang, J. Power Sources 129 (2004) 101.